AT file

AT/17.2.1/001

The optimum length of the AT spur

Ray Norris

17 October 1984

1.0 SUMMARY

It has been shown (AT/17.2.1/001) that a North-South spur added to the compact array (CA) of the AT would significantly improve the performance of the CA at low absolute declinations. For the simulations in that report, a spur length of 1km was assumed. It has since been requested that some simulations be run to determine the optimum length of the spur. This report presents the results of those simulations, and shows that a spur length of 1km is indeed approximately optimum, although flexibility should be provided to increase this length in the light of possible future astronomical considerations.

2.0 INTRODUCTION

In the original AT plan, an E-W array (with its inherent poor performance at low absolute declinations) was chosen since there seemed little point in competing with the VLA, which already maps equatorial sources adequately. However, the AT is planned to operate at frequencies which are not implemented at the VLA. Thus the need arises for better uv coverage at low absolute declinations, and this may be obtained by the addition of a short N-S spur added to the E-W array. Therefore the spur is likely to be of most use for mapping equatorial sources at the high frequencies not implemented on the VLA. There is a prevalent assumption that few astronomical sources show compact structure at these high frequencies, other than ultra-compact objects such as SiO masers and flat-spectrum galactic nuclei. Thus the shorter configurations are probably of most importance, although discovery of compact high frequency structure (e.g. molecular jets) by the AT would necessitate revision of this assumption. The shortest configuration for which the AT stations are optimised is the 1.5km array, and so the simulations presented here have all been run using a 1.5km basic array.

3.0 THE PARAMETERS OF THE SIMULATIONS

Each simulation was run using an 8 day observation of the source SPIRALL using the array DR1D4 to which a spur was added at the 2.25km point. The data were uniformly weighted, gridded, and inverted, and then CLEANed for 9000 iterations using a loop gain of 0.2 and no stabilisation spike. As in AT/17.2.1/001, an additional telescope was used on the spur to avoid disruption of the optimised DR1D4 array, and so the observations simulated here might take about 9 days in practice, assuming that a telescope would be moved onto the spur from the E-W array.

Simulations were run for spur lenghths of 0, 0.5, 1.0, 1.5, and 2.0km. The 0km array is identical to the basic DR1D4 array, and the 1km array is identical to array 7 of AT/17.2.1/001. For each array, the spur telescope was moved one eighth of the spur length each day to reach its maximum baseline on day 8.

4.0 RESULTS

The resulting uv distributions are shown in Figure 1 and the resulting maps in Figure 2. It is clear from Fig. 2 that any length of spur ≥0.5km results in a dramatic improvement of the maps at low absolute declinations. The differences between the spur lengths are less clear cut, but the following effects are noticeable:

1. The maps at declination -60° appear to get slightly 'noisier' as the spur length increases. This is reflected in the upper graph of Figure 3, which shows the dynamic range slightly decreasing with spur length. This seems to be an artefact of the mapping process, and results from a slight reduction of the peak intensity.

2. The maps at declinations -30° and -10° get considerably noisier as the spur length increases. The upper graph of Figure 3 shows the dynamic range decreasing significantly with spur length, although it remains higher than the dynamic range attained with no spur. Only a small part of this effect is attributable to the artefact mentioned above. Most of the effect is instead attributable to reduced filling of the uv plane in the regions to the immediate North and South of the tracks of the E-W telescopes. This effect therefore limits the maximum useful length of the spur.

3. All maps, and particularly those at low absolute declinations, show a reduction in the amount of N-S elongation and artefacts as the spur length increases. This is of course due to the increased maximum N-S baseline, and limits the minimum useful length of the spur. This is reflected in the bottom graph of Fig. 3, which shows the fidelity increasing with increased spur length.

5.0 THE OPTIMUM LENGTH OF THE SPUR FOR A 1.5KM ARRAY

The optimum length is determined by effects 2 and 3 above, and represents a choice of the best compromise. This optimum length clearly lies somewhere between 0.5 and 1.5km, but does not seem very critical. The nominal length of 1km which was originally chosen is probably a good approximation to the optimum length.

6.0 THE OPTIMUM SPUR LENGTH FOR OTHER ARRAYS

6.1 The 3km and 6km arrays

The result here can presumably be scaled roughly to give optimum spur lengths of 2km and 4km for the 3km and 6km arrays respectively. However, the main use of the spur is likely to be for high frequency observations, in which it is probable that the shorter arrays would be more useful. Ultimately, the decision on whether to extend the spur for the longer arrays will depend on:

1. Whether there are interesting astronomical structures which are unresolved by the 1.5km array but would be resolvable by the 3km or 6km arrays, and

2. Whether the high cost of laying extra rail track and stations could be funded from the available budget.

The first of these criteria must await astronomical information which is not currently available, and which will not be available until the completion of the AT. Thus we are not presently in a position to decide on the usefullness of a spur for the longer arrays.

6.2 The 750m array

No adequate simulations have yet been done for the E-W 750m array (although some are in progress), and so it would be premature to simulate the effect of a spur on this array. However, scaling the results for the 1.5km array implies that a 0.5km spur would be optimum for the 750m array. Such a spur could be provided by placing extra stations along the first 500m of the 1km spur. At this stage, it is necessary only to determine the position of the rail track: individual station locations do not yet need to be known. The impact of the 750m array upon the spur length may therefore be ignored for the time being.

7.0 CONCLUSION

The spur is likely to be of most use for mapping equatorial sources at frequencies not implemented on the VLA. At these high frequencies, the shorter configurations are probably of most importance, although discovery of compact structure by the AT would necessitate revision of this assumption. The shortest configuration for which the AT stations are optimised is the 1.5km array, and for this a spur length of about 1km seems to be optimum.

This length is not, however, critical, and financial constraints may restrict the length without degrading the performance too seriously. On the other hand, discovery of compact high frequency structure by the AT might imply that an even longer spur would be necessary. Thus, for the present, an optimum working plan might be to adopt a nominal spur length of 1km, whilst retaining the option of lengthening it (for astronomical reasons) or shortening it (for financial reasons).

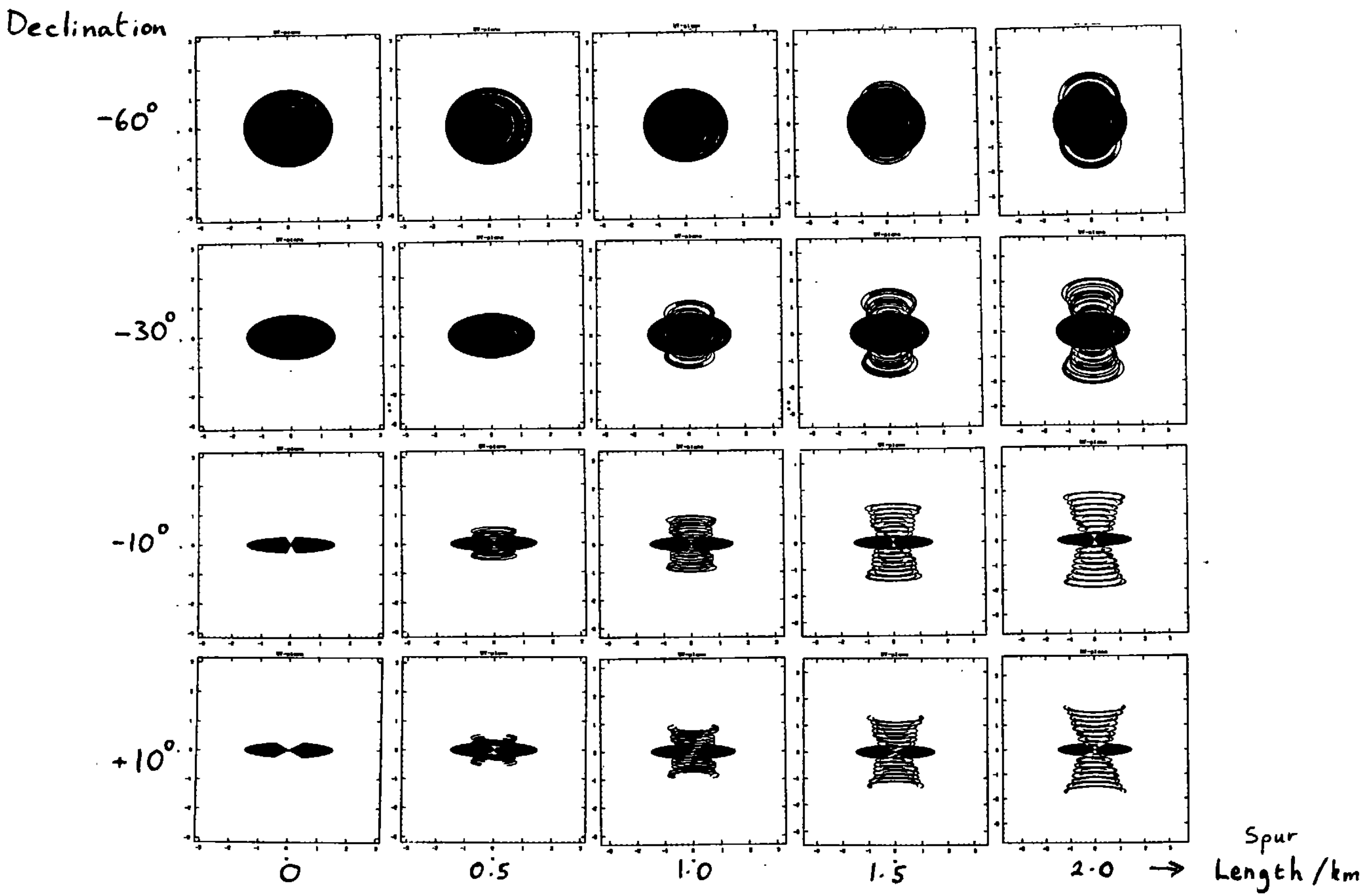

Figure 1 UV coverage of the arrays. Each array consists of the basic 1.5km E-W array DR1D4, to which a spur of the length shown has been added at the 2.25km point. The uv plots show all baselines between all telescopes over the 8 days of observation.

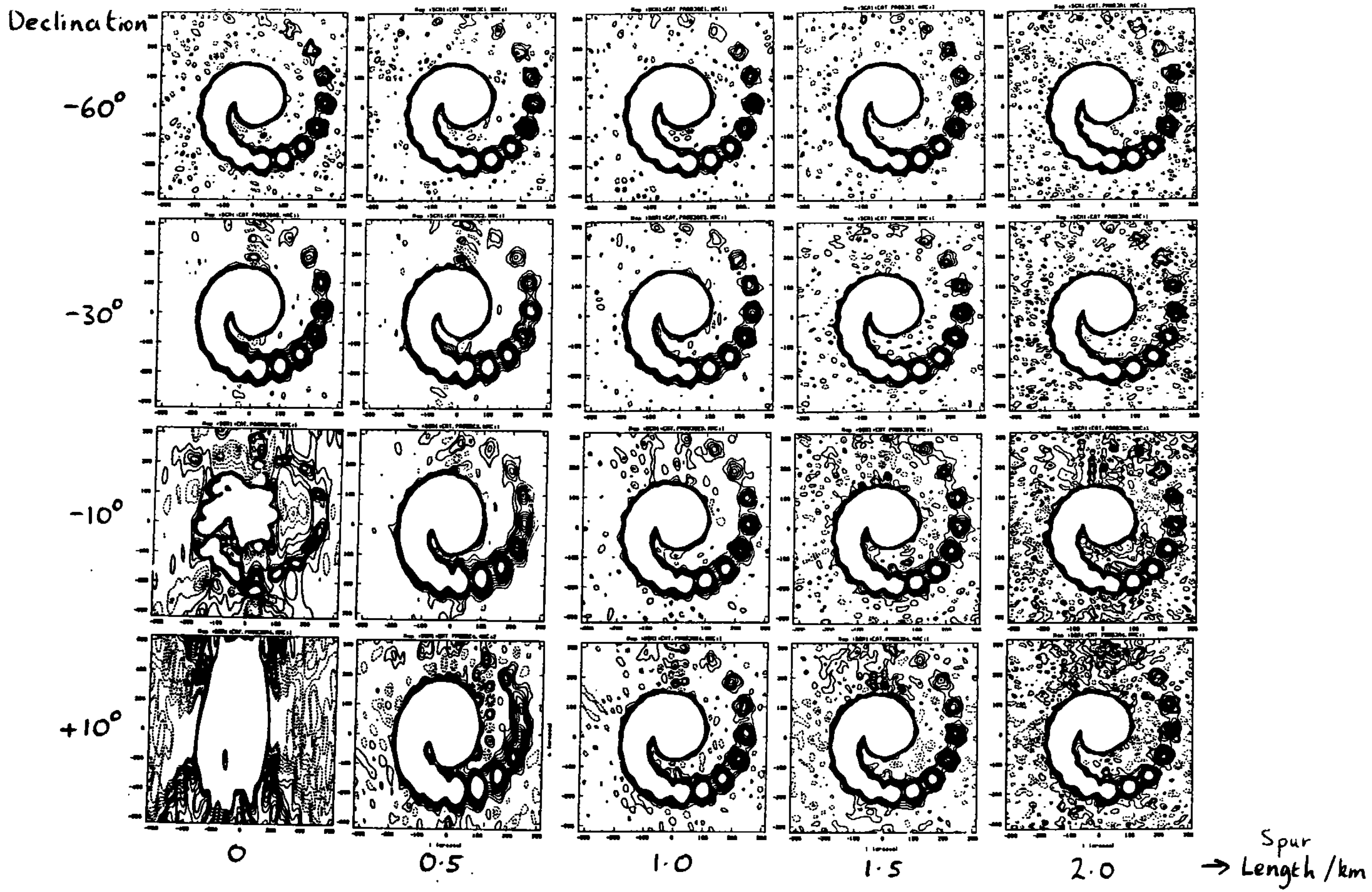

Figure 2 The CLEANed maps resulting from the simulations. Contours are at intervals of 0.02% of the peak intensity.

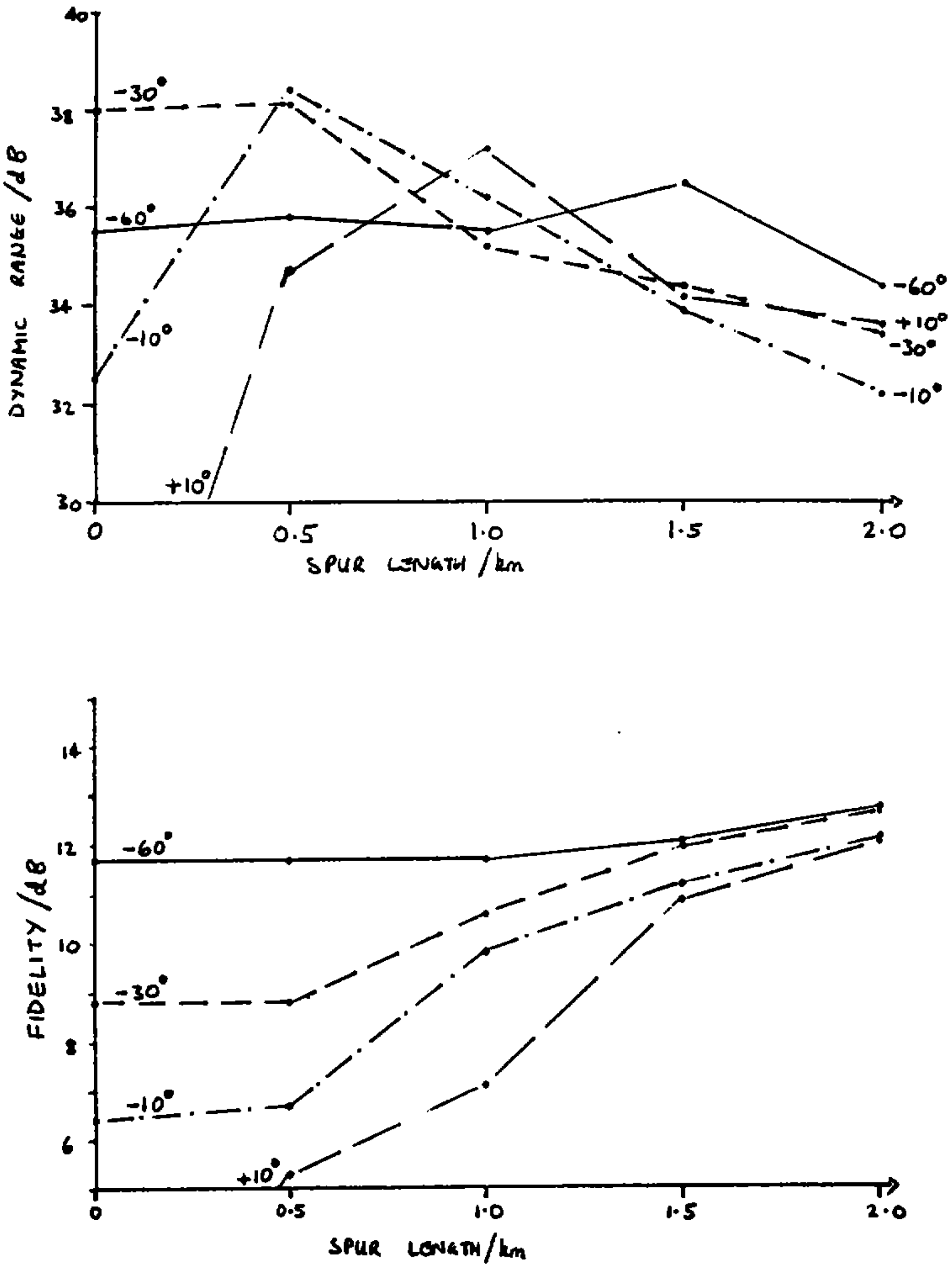

Figure 3 Plots of the dynamic range and fidelity of the maps as a function of spur length. Dynamic range and fidelity are defined as in AT/17.2/003.

TECHNICAL ADVISORY GROUPS
CONFIGURATION STUDY GROUP
TECHNICAL NOTES AND REPORTS
AT/17.2.1/001

A Spur for the AT Compact Array

R.P.Norris

19 July 1984

1.0 INTRODUCTION

It has ben suggested that a short N-S spur might be added to the compact array of the AT at some point in the future. The motive for this suggestion is that the E-W configuration of the AT compact array is unsuitable for low absolute declinations, but this could be rectified by the addition of a N-S spur. Although this plan remains no more than a possibility, it is important at this stage to decide where such a spur is best placed, in order that placing of structures now does not preclude optimum placing of the spur in the future. This note presents the results of a series of simulations which were run in order to locate the optimum position of the spur.

2.0 PARAMETERS OF THE SIMULATIONS

The starting point for the simulations were the 6km array DR6D4, the 3km array DR3D4, and the 1.5km array DR1D4. To these were added a series of spurs in different configurations. In each spur, an extra telescope was used, rather than moving an existing telescope from the 3km track. The reason for this was that the E-W arrays had been optimised to maximise uv coverage, and this optimisation could not easily be repeated to include each spur. Instead, the resulting extra sensitivity from the spur telescope is completely equivalent to what could be obtained by moving a telescope on to the spur from the 3km track, and then observing for an extra day to fill in the missing uv spacings. As will be seen, this discussion is somewhat academic since the maps are generally limited (at the low absolute declinations of interest) by uv coverage rather than by sensitivity.

In each case, simulated sources were observed at a range of declinations, at a frequency of 1.4GHz, for a period of 8 days. The data were gridded using uniform weighting, transformed and convolution corrected, and then cleaned using 9000 iterations at a loop gain of 0.2. No stabilisation spike was used during cleaning.

3.0 THE ARRAYS

The simulated arrays are shown in Figure 1. Array 0 is the one dimensional array which could be configured as DR1D4, DR3D4, or DR6D4, depending on which sections were used.

Arrays 1, 2, 4, and 5 use a single telescope at a distance of 1km North of the E-W array. These arrays were included to see if a reasonable result could be obtained using a single telescope rather than a section of track with a movable telescope. The difference between arrays 1 and 2 is small. Array 1 has the telescope 1km N of E-W station 109 (at a distance of 1.635km from the end of the array), whereas array 2 has it 1km N of the 1.5km central point. Simulations subsequently showed that changes of this scale have no significant effect on the maps.

Arrays 3, 6, and 7 use a 1km N-S track with 8 equidistant stations along it. For these arrays, the telescope was started at the station closest to the E-W track, and moved one station each day, so that on day 8 it was 1km N of the E-W track. The significance of array 7 is that the spur is at the mid-point of the 1.5km array.

It should be noted that all the arrays place the spur to the North of the E-W track. However, symmetry argues that the results would be identical if the spur were placed to the South.

4.0 INTERPRETATION OF THE RESULTS

To evaluate the results from the different simulations, a variety of figures-of-merit were tried, with little success. It seems that such quantities are unreliable for sparsely filled or irregularly filled uv diagrams.

The dynamic range and fidelity (as defined in AT/10.1/036) were also measured for each map produced, but, although these corresponded roughly to the subjective appearance of the maps, they were found to be unreliable. This is because the dynamic range depends on exactly which components, or artefacts, appear in the region being monitored, and the fidelity 'saturates', because of the slight broadening produced by CLEAN. It was therefore decided that the best measure of the quality of a map was its subjective appearance.

5.0 RESULTS USING THE 6KM ARRAY

Simulations were run simultaneously on the 3km and 6km arrays, and it was quickly apparent that the effect of the spur on the 6km simulations was very much less pronounced than on the 3km array, and that the position of the spur was not critical for the 6km simulations. The 6km simulations were therefore discontinued in favour of the shorter arrays.

6.0 RESULTS USING THE 3KM ARRAY

Figure 2 shows the results of the 3km simulations. It is immediately apparent that:

1. The addition of any spur makes the array usable at declinations as high as $+10^{o}$, whereas without the spur the array becomes unusable near the celestial equator. Other simulations in fact showed that usable low dynamic range maps could be obtained at declinations as high as $+30^{o}$.

2. The resulting maps for arrays 3, 6, and 7 are very much better than those for arrays 1, 2, 4, and 5. It may be concluded that the use of a spur section of track, rather than a single telescope located at 1km N, is a worthwhile investment.

3. The difference between arrays 3, 6, and 7 is not conspicuous in the maps. More detailed investigations of the maps showed that the map resulting from array 3 was slightly better than those from arrays 6 and 7.

7.0 RESULTS USING THE 1.5KM ARRAY

As expected, the 1.5km simulations were more sensitive to the position of the spur than were the 3km simulations, and so the results are shown in rather more detail. Figure 3 shows the uv tracks for the simulations, and Figure 4 shows the resulting maps. It is clear that arrays 3 and 7 give better results than array 1. Formally, the results from array 7 are comparable with those from array 3. N-S artefacts are apparent on some maps from array 7, whilst maps from array 3 show a SE-NW elongation. However, it may be argued that the artefacts from array 7 are preferable to those from array 3 because the effect of the array 3 artefacts will depend strongly on source structure and orientation, and may give misleading results. On the other hand, array 7 artefacts, being N-S, are clearly recognisable as such. In addition, the array 7 maps at high negative declination are somewhat better than the corresponding array 3 maps, because the uv coverage is more nearly circular.

In conclusion, the 1.5km simulations favour a spur track at the 2.25km point. This position is also suitable for the 3km and 6km arrays.

8.0 SIMULATIONS OF OTHER SOURCES

Informal presentations of these simulations have provoked some surprise that the array with a simple spur could perform so well so near the celestial equator, and the question of whether this result is source-dependent has been posed. Some simulations have therefore been run on more complex and extended source structures.

Figure 5 shows the results of simulations on the source ZYGNUS, which has both extended and narrow structures. No map is shown for the DR3D4 array (array 0) at declination $+10^{\circ}$, because CLEAN crashed with an overflow when processing this data! The bottom row shows that the addition of a spur (array 3) allows this source to be mapped successfully at declinations up to $+10^{\circ}$.

Figure 6 shows the results of simulations on the extended emission of the source VIRGO. Again, it was not possible to map this at all at declination $+10^{\circ}$ with array 0, whereas array 3 (centre row) produces usable map at declinations to $+10^{\circ}$ The bottom row was mapped using array

6, which gave poorer results on the source SPIRAL. In this case, however, array 6 seems to produce comparable (or arguably better) results to those from array 3, and this is presumably attributable to the orientation of this particular source. However, it is not recommended that we match the array configuration to the orientation of our favourite sources.

9.0 CONCLUSION

The simulations presented here have shown that the optimum location for the spur is at the 2.25km point of the E-W track, and should consist of a N-S track with a number of stations along it. The exact location of these stations (and possible departures from a N-S orientation) have not been investigated in these simulations.

The exact position is not critical, the main requirement being that the spur should be situated close to the centre of the 1.5km array. Furthermore, it is immaterial, from an astronomical viewpoint, whether the spur lies to the N or to the S of the track.

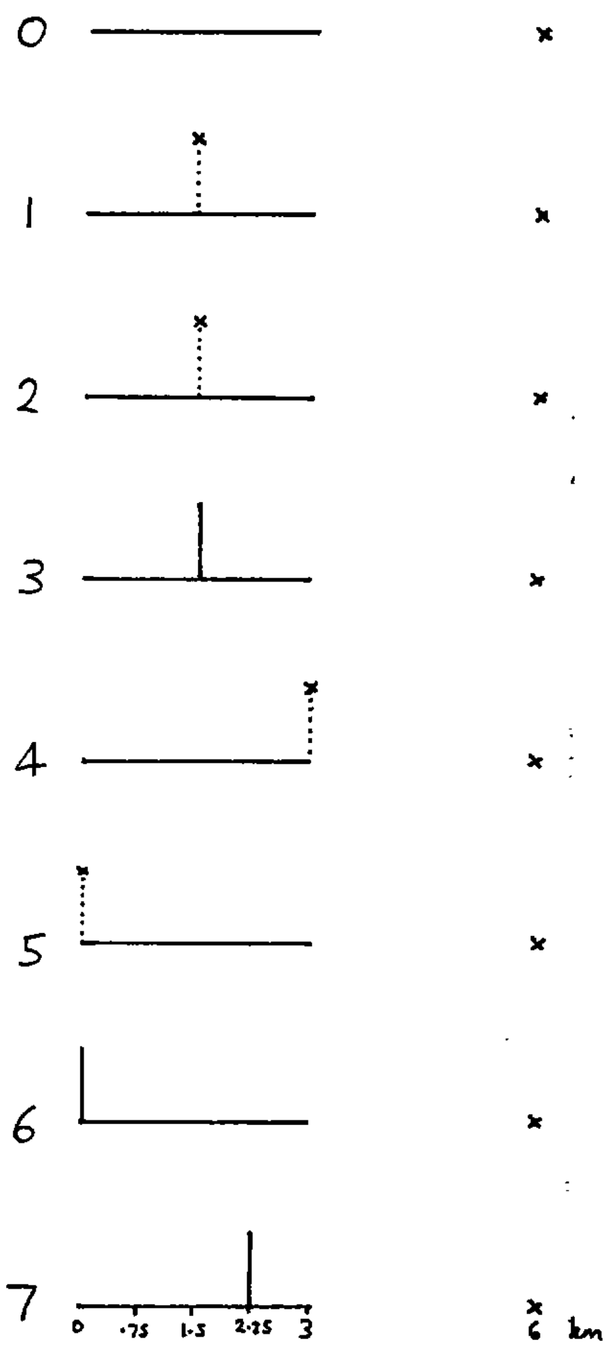

Figure 1 The arrays used for the simulations. Array 0 is the basic E-W array, which may be configured as DR1D4, DR3D4, or DR6D4. Array 1 shows the addition of a single telesope 1km N of station 109 (1.635km), whereas array 2 shows the addition of a single telescope 1km N of the 1.5km position. Array 3 shows a 1km track, with 8 stations along it, at the 1.5km point. Arrays 4 and 5 respectively show the addition of a single telescope 1km N of each of the two ends of the 3km E-W track. Array 6 shows a 1km spur track, with 8 stations, situated at one end of the 3km track, and array 7 shows the track situated at the centre of the 1.5km array.

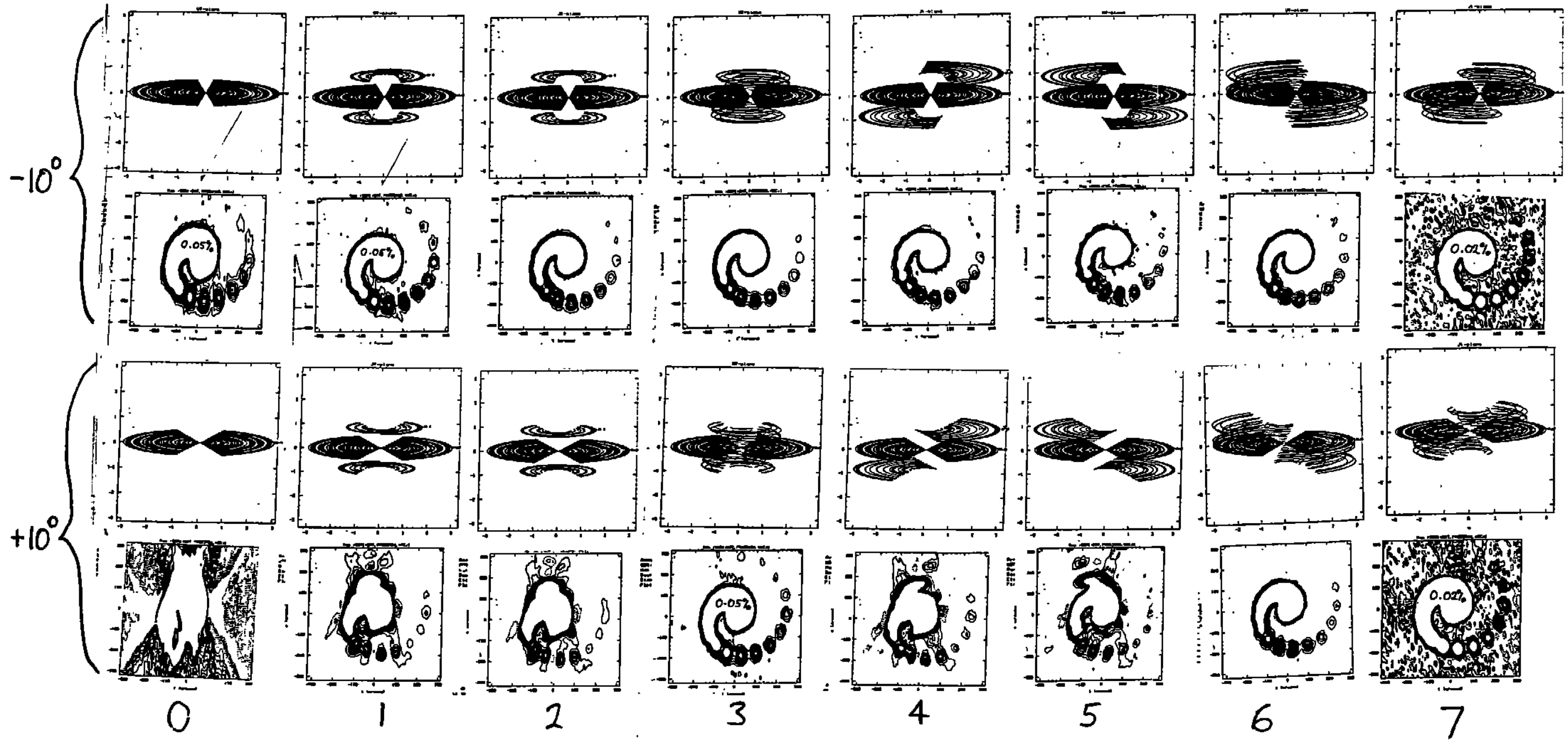

<u>Figure</u> <u>2</u> Simulations of the source SPIRAL at declinations $\pm 10^\circ$. Each map is plotted with contour intervals of 0.1%, except where stated otherwise. The numbers along the bottom refer to the different array numbers.

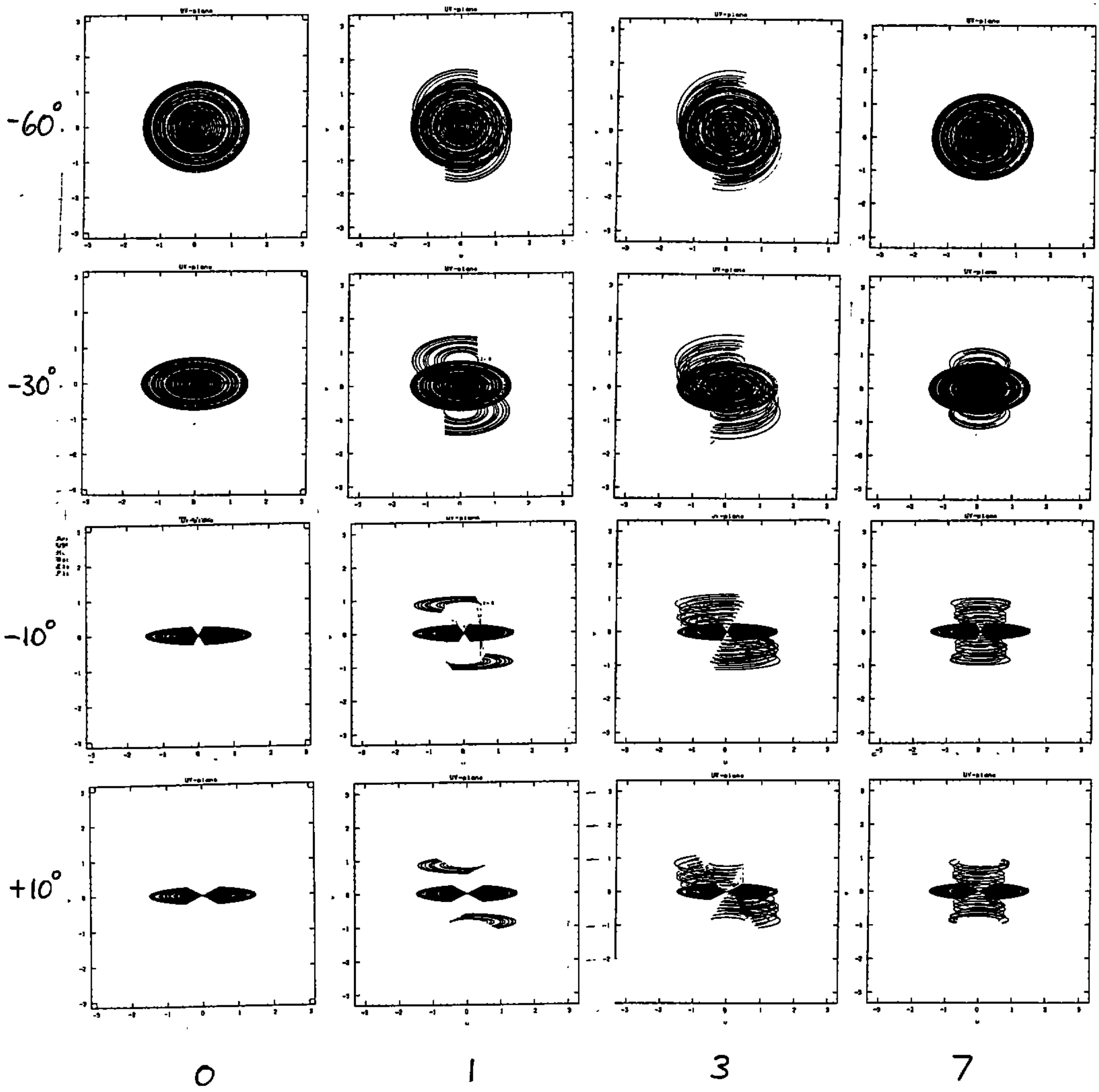

Figure 3 UV distributions for the 1.5km array simulations, for four different arrays and four declinations. The corresponding maps are in Figure 4.

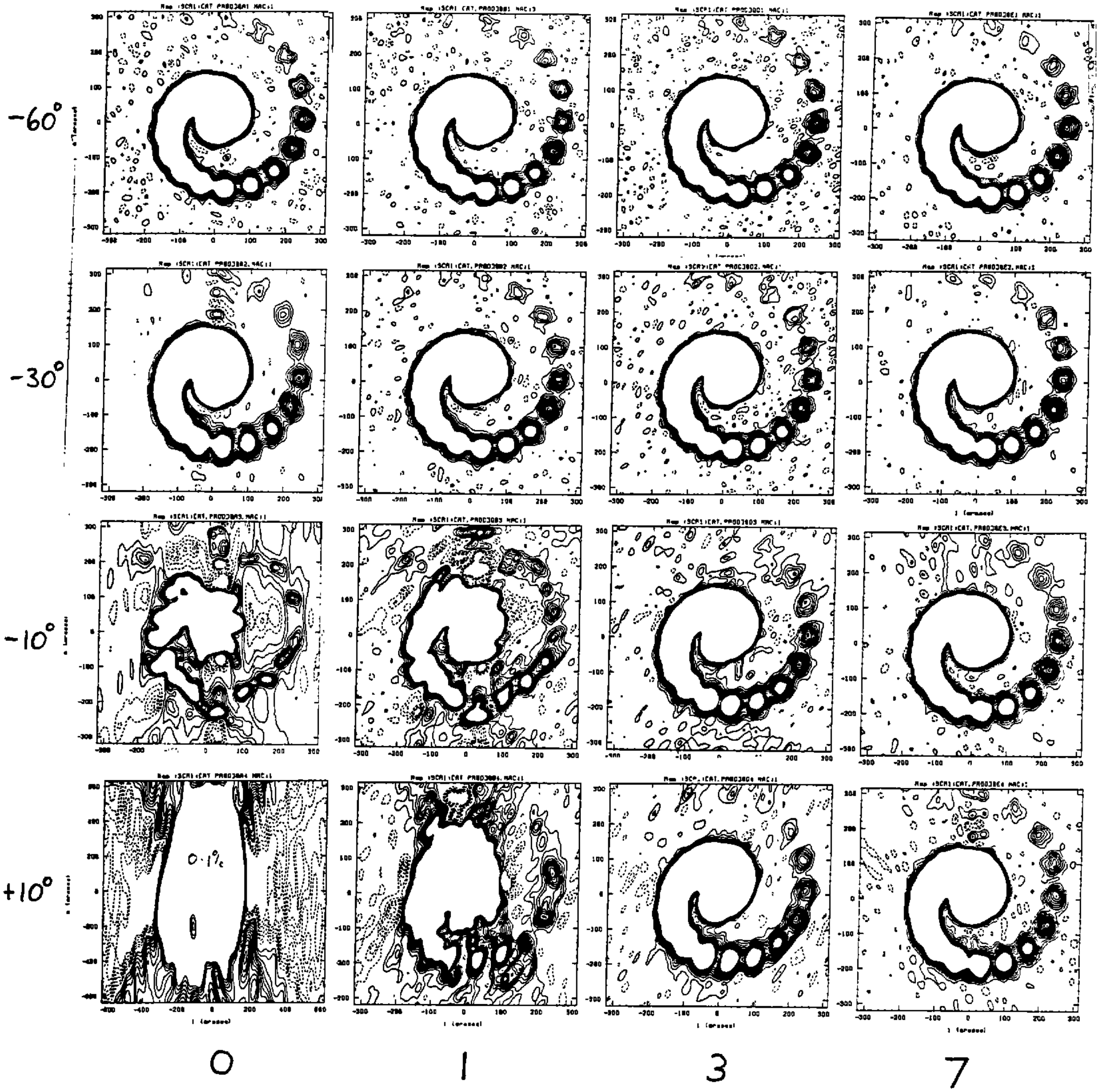

Figure 4 Simulated maps of the source SPIRAL at four different declinations with four different arrays. The corresponding uv distributions are shown in Figure 3. Each map is plotted with contour intervals of 0.2%, except whre stated otherwise.

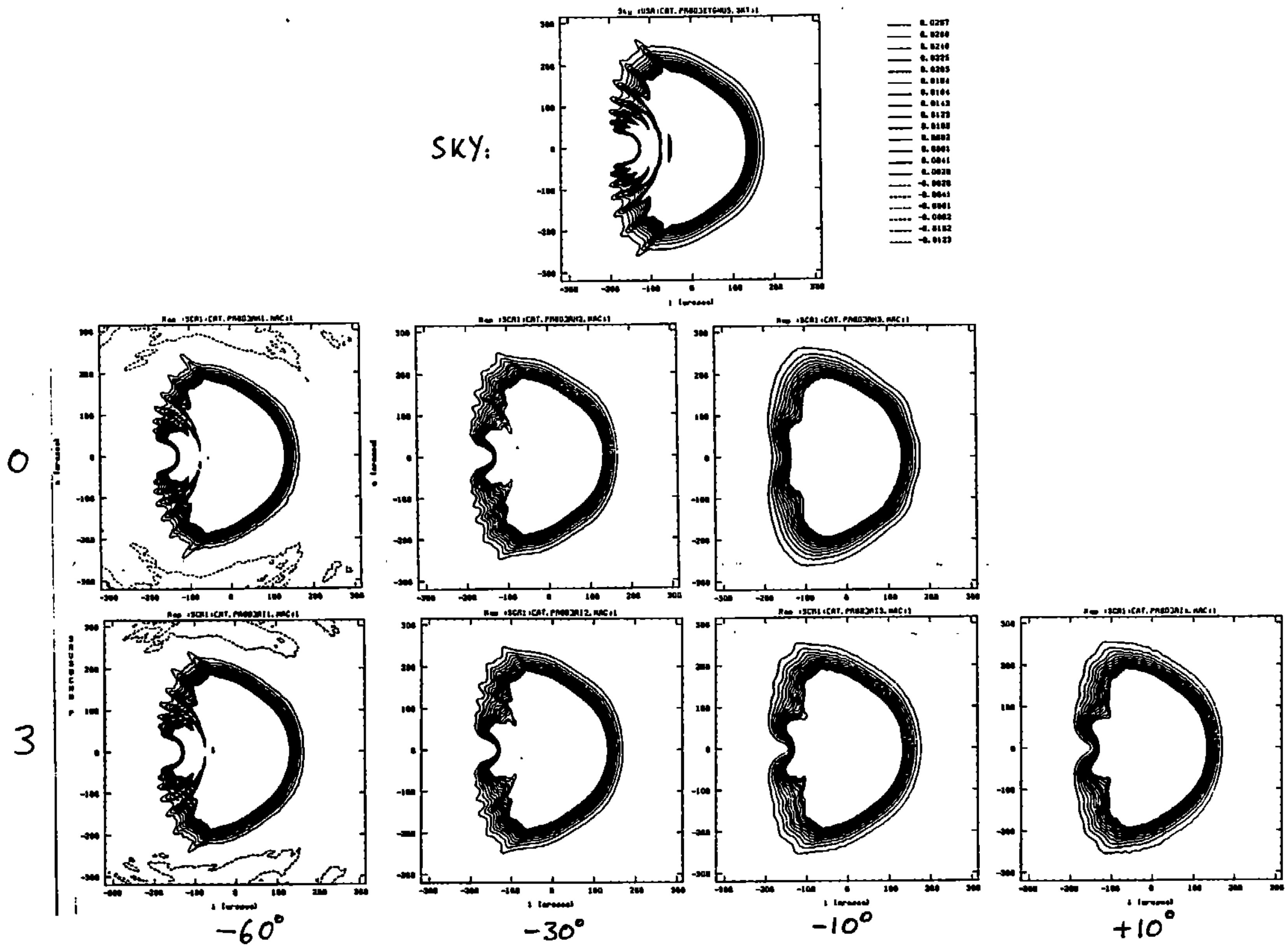

Figure 5 Simulated maps of the source ZYGNUS. The top map shows the 'sky' distribution. The top row shows simulated maps obtained with array 0 at declinations -60°, -30°, and -10°. CLEAN was unable to cope with the array 0 data for +10°. The bottom row shows the simulated maps obtained with array 3. All maps are plotted at contour intervals of 1%.

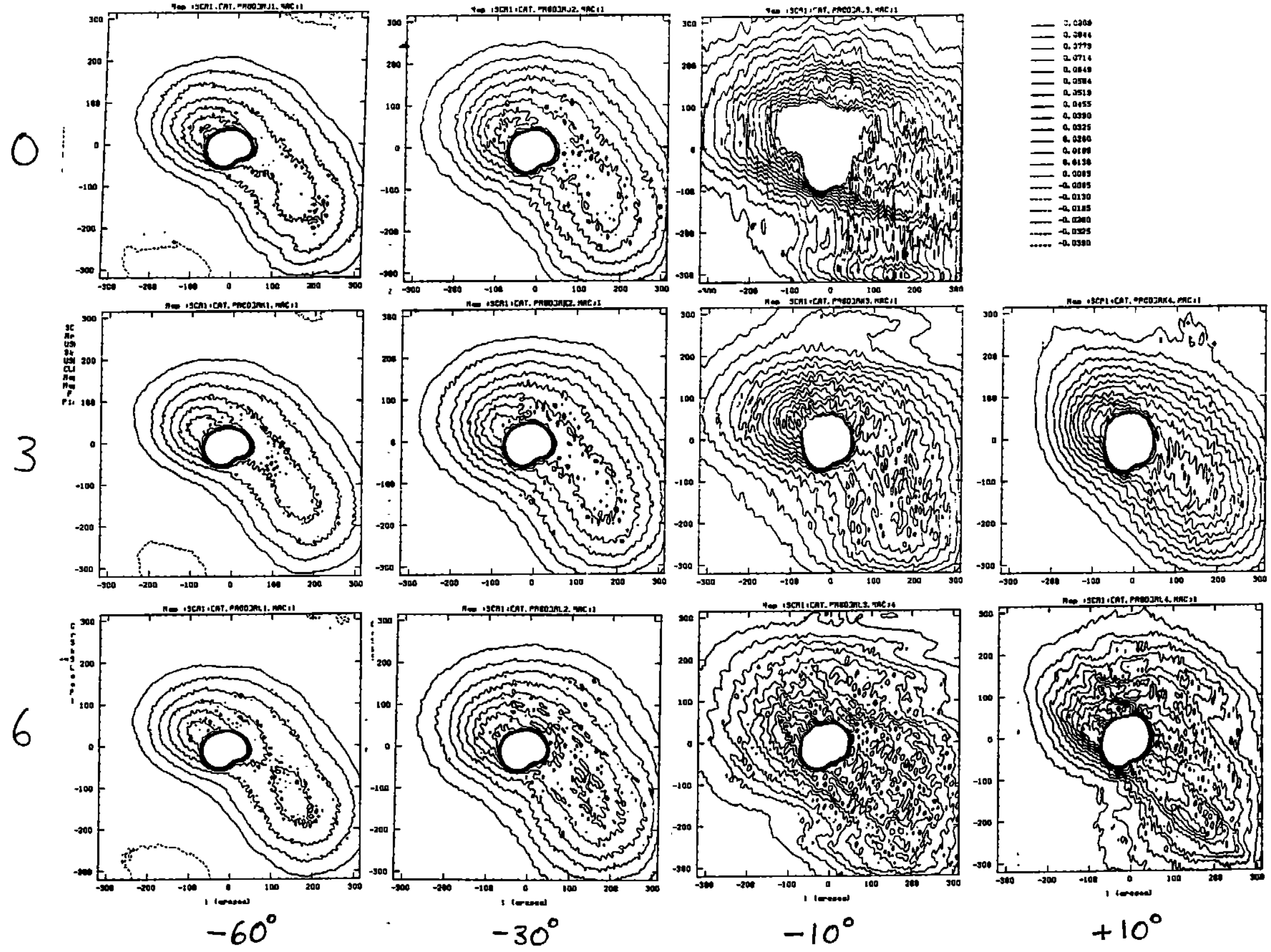

<u>Figure</u> <u>6</u> Simulated maps of the source VIRGO. The top row shows maps obtaiend from array 0, the middle row from array 3, and the bottom row from array 6. As in Figure 5, CLEAN was unable to cope with the array 0 data for declination $+10^{\circ}$. All maps are plotted at contour intervals of 0.1%.